CLUSTERS AND NUCLEAR FLOW

W. REISDORF
GSI, Planckstr. 1
64291 Darmstadt, Germany
E-mail: W.Reisdorf@gsi.de

FOPI Collaboration

We discuss clusterization in central heavy ion collisions in the energy range between 90 and 400 A MeV. Pronounced system-size dependences are observed for participant matter. Possible correlations with size-dependences of sideflow, pion multiplicity and momentum space topology are pointed out. A mixing experiment is described that demonstrates the importance of non-equilibrium dynamics.

1 Introduction

One of the surprising phenomena recently observed [1] in *central* Au on Au collisions at intermediate energies, is the large probability of emitted protons to appear within 'clusters' rather than as single nucleons. Fig.1 shows that the probability of participant protons to attach themselves to at least one other nucleon at 'freezeout' time, is as high as 80% at 150A MeV and still roughly 50% at 1A GeV.

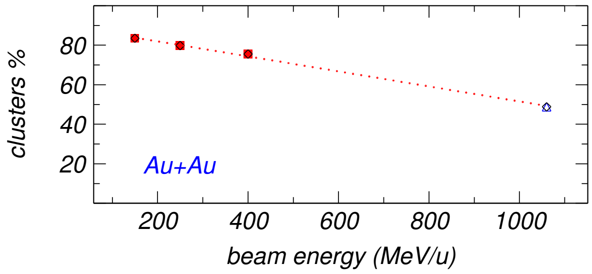

Figure 1: Excitation function for the proton clusterization probability in central Au+Au collisions

In the energy range primarily discussed here (90-400A MeV) the available c.o.m. energy varies from 22 to 95A MeV, well beyond the known binding energy of 8A MeV for stable nuclei. The survival of so many clusters in this energy regime calls for models that go beyond naive global statistical equilibration concepts. The observation [2,3,1] of pronounced mass-dependences of the kinetic energies was interpreted as evidence for strong radial flow caused by an expansion of the hot and possibly initially compressed fireball. Such scenarios could be used to understand [3,1] the kinetic energy spectra of the emitted clusters, as illustrated in Fig.2. The energy taken up by such an expansive flow was estimated to be as high as 60%. At 250A MeV incident energy, to be specific, this still meant that about 20 MeV per nucleon (the Q-values are about −5A MeV) were available for 'local use'. It is therefore not surprising that statistical multifragmentation calculations, allowing for the available *local* energy, still failed to reproduce the measured fragment yields as illustrated in Fig.3. To obtain fair agreement with the data one has to assume that the primary fragments are cold, in obvious contradiction to statistical expectations.

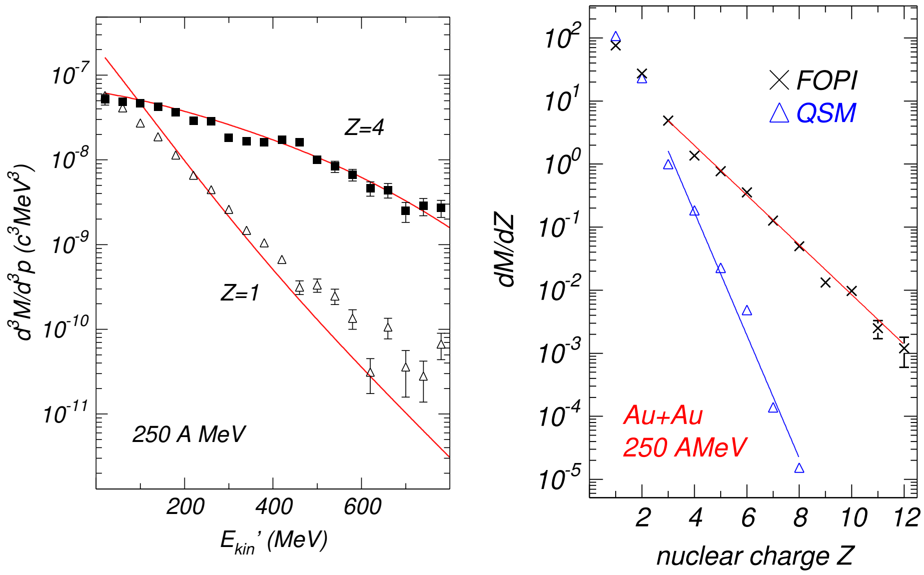

Figure 2: Left panel: kinetic energy spectra of Z=1 and Z=4 fragments emitted in central Au on Au collisions near 45° (c.m.). The smooth curves are blast model fits. Right panel: Fragment charge distribution. Comparison of the experimental data (× FOPI) with constrained statistical model predictions (△).

In the following we discuss new, partially preliminary results obtained by the FOPI Collaboration, that shed additional light onto this complex subject. A theoretical approach is presented by A. Ono [4].

2 Observation of system-size dependences

Our Collaboration uses a 4π detector [5] which is located at the SIS/ESR accelerator facility of GSI, Darmstadt, and which allows to identify Light Charged Particles (LCP), Intermediate-Mass Particles (IMF), as well as produced particles, such as pions and kaons, using a combined magnetic rigidity, time-of-flight and energy-loss analysis

It is of interest to study the system-size dependence of multifragmentation and its possible correlations with other observables. In Fig. 3 we compare the IMF multiplicity in the system Au+Au with that for Ni+Ni.

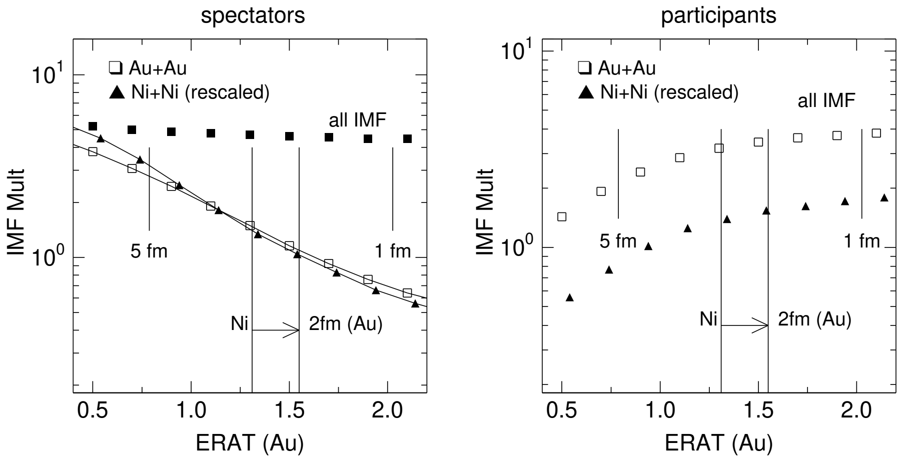

Figure 3: IMF multiplicities in spectator (left) and participant (right) matter for Au+Au and Ni+Ni as a function of ERAT, see text.

To remove trivial size dependences we have scaled the Ni data by 79/28, the ratio of projectile charges in the two symmetric systems. We vary the centrality using as global event selector ERAT, the observed ratio of total transverse to total longitudinal kinetic energy. For the Au+Au system the geometrical interpretation of the cross sections (in fm) is indicated in the figures. In the left hand panel we compare 'spectator' sources, somewhat arbitrarily defined as originating from scaled rapididities $|y^{(0)} \pm 0.4|$. For projectile (target) $y^{(0)} = 1$ (-1). We find that the (scaled) IMF multiplicities of the Ni system are very close to those observed in the Au system, independent on the event selection. Note that the abscissa (ERAT) has been shifted for the Ni system, as shown in the figure in order to overlay data belonging to the same reduced impact parameter b/b_{max}, b_{max} being the maximum (grazing) value of b. This size-independence is in line with the universality of spectator fragmentation observed by the ALADIN collaboration [6].

The right panel of Fig. 3 shows that outside the spectator rapidities, universality is lost: at comparable reduced impact parameter about twice as many IMF's *per nucleon* are created in the heavier system, again very weakly dependent on ERAT, i.e. the centrality. For participant matter we are here in an energy region where the IMF multiplicity is expected to decrease with increasing available excitation energy: hence, applying thermal language, we can say that the heavier participant system appears to be colder.

Is there a correlation with other observables? It turns out that size dependences are also seen for sideflow, Figs. 4,5, the scaled pion multiplicity, Fig. 6, and the momentum-space topology of events with the same centrality, Fig. 7.

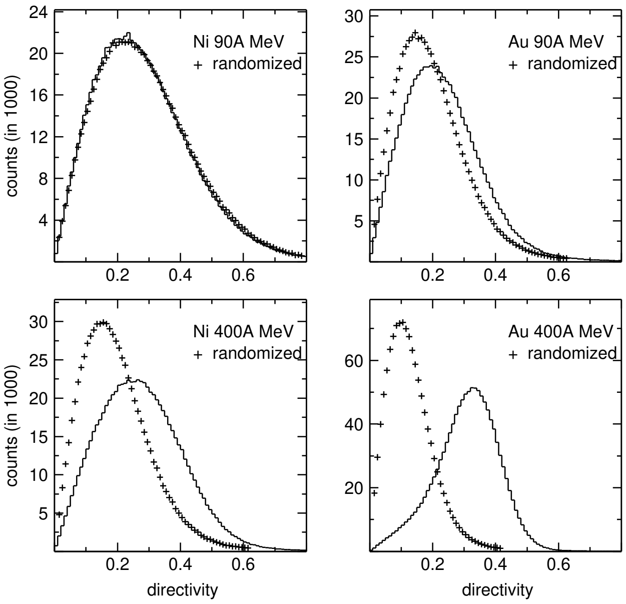

Figure 4. Directivity distributions (histograms) for various systems and energies indicated in the panels. Randomized distribution (crosses) are shown for comparison.

Briefly, in Fig. 4, we present distributions of the directivity D defined by

$$D = \frac{\sum sign(y)\, \vec{p_t}}{\sum |p_t|} \tag{1}$$

where $sign(y)$ is $+1$ in the forward hemisphere and -1 else and the sums are taken over all observed particles. The directivity is a good measure for sideflow. The data shown are integrated over a broad range of impact parameters, $b < 0.5\, b_{max}$. As all observables are subject to finite-size fluctuations, it is important to remove this effect before drawing conclusions on non-trivial system-size dependences. The random walk distributions of D (crosses), obtained by randomizing the azimuthal emission angles in each event, are compared with the actual distributions (histograms).

One finds that the random distributions of this scale-invariant observable are broader for lighter than heavier systems (i.e. the *relative* fluctuations are larger), see the top two panels in Fig. 4, and narrow down at higher energies because of increasing particle multiplicities (compare the top with the bottom panels). Comparing with the actual distributions one sees that
1) At 90A MeV there is no net effect for the Ni system, while a statistically significant signal is seen for Au.
2) At 400A MeV sideflow has increased substantially in both systems.
3) The sideflow excitation function, Fig. 5, after correction for the finite number fluctuation, shows a dramatic system-size dependence.

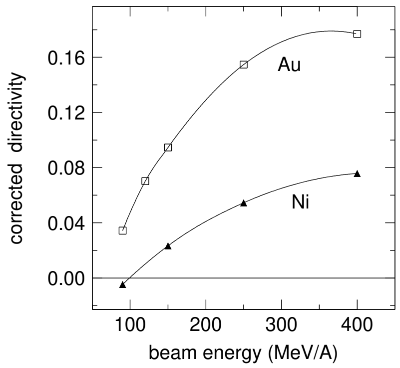

Figure 5: Excitation function of the finite-size corrected directivity for Au+Au and Ni+Ni

While flow is naturally understood using hydrodynamical considerations, this observation is incompatible with the expectations from ideal one-fluid dynamics which relies on complete local equilibration.

Mid-rapidity pion transverse 4-velocity spectra (scaled with the projectile 4-velocity) are shown in Fig.6 for both systems, Ni and Au. While the ratio of π^+/π^- multiplicities is higher for the Ni system due to a higher proton/neutron ratio in this system, it is clear that the sum of pions emitted by the lighter system is larger: again, the Ni data have been scaled with 79/28 and normalized to the same number of events.

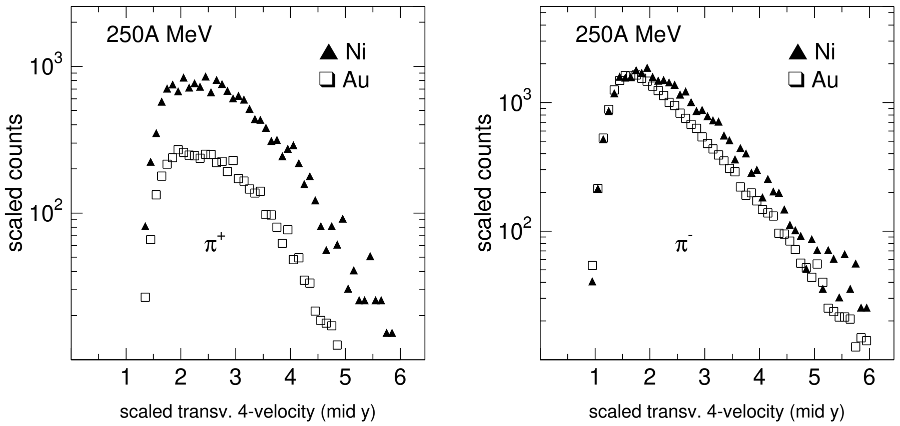

Figure 6: Mid-rapidity transverse 4-velocity spectra of pions (π^+ left, π^- right) for Ni+Ni and Au+Au at 250A MeV.

Finally, from Fig. 7, we read off that the momentum-space topology is more elongated in the lighter Ni system. The fact that transverse momenta are larger in the chemically 'colder' system (Au+Au) is remarkable. It suggests again that a sizeable amount of these momenta are in *ordered* motion, or radial flow. But in addition the size dependence tells us that the development of such flow requires a minimum amount of *bulk* material, not available in light systems, where surface effects dominate. But since we have seen earlier that a *locally* equilibrated fluid dynamics scenario seems to fail quantitatively, we are still left with the question of how to assess non-equilibrium effects.

3 Observation of incomplete mixing

We have performed an experiment that allows to detect non-equilibrium effects more directly. At 400A MeV we studied the isospin-asymmetric, but mass-symmetric system ^{96}Zr + ^{96}Ru. The results are summarized in Fig.8. The left panel shows for highly central collisions the observed yields of protons plus deuterons as a function of the center-of-mass angle θ_{cm}, the right panel displays the observed t/^{3}He ratios as a function of centrality (increasing from left to right), in a fixed rapidity bin ($y^{(0)} = 0.25 - 0.75$). As ^{96}Zr and ^{96}Ru differ only by 4 protons (or 10%), one has to make some additional effort to judge quantitatively if complete mixing of projectile and target nucleons has taken place.

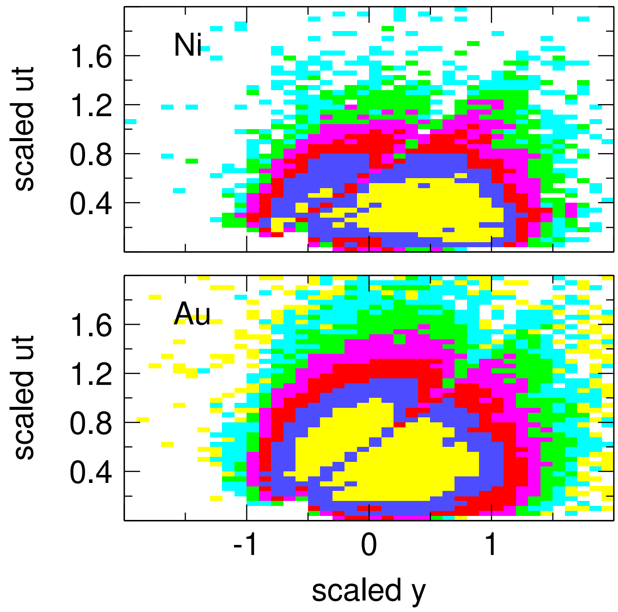

Figure 7: Momentum space distributions of Li fragments in central Ni+Ni (top) and Au+Au (bottom) collisions at 250A MeV

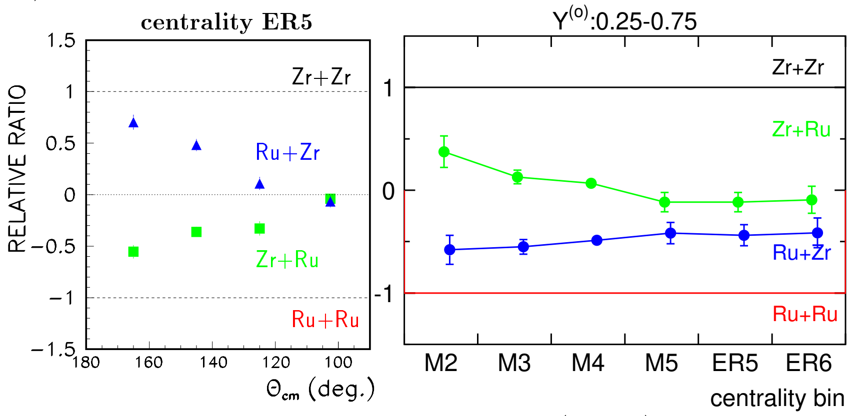

Figure 8. Left: Proton counting as a function of polar angle (see text). Right: Normalized triton/^{3}He ratio as a function of increasing centrality.

One repeats the same measurements for the completely symmetric systems ^{96}Zr + ^{96}Zr, respectively ^{96}Ru + ^{96}Ru to obtain reference values of the studied observables, which for convenience were normalized to +1 (Zr), resp. (-1) (Ru) in the figures. Furthermore, to overcome apparatus asymmetries one inverts also target and beam in the asymmetric combination.

In Fig. 8 the mixed systems should meet at some constant common intermediate value if complete mixing had been achieved in phase space. They do so only at 90° in the c.o.m. where, *by principle*, incomplete mixing cannot be tested. This experiment has therefore shown unambiguously that mixing equilibrium has not been achieved. For more details see refs. [8].

4 Conclusion

To summarize, the heavier system apears to be be 'chemically colder': more clusterization, less pions; it has larger sideflow and higher transverse momenta. If one interpretes the latter as indicative of higher *radial* flow, one is tempted to conclude that flow is cooling the system, as one would expect qualitatively from an adiabatic expansion scenario. On the other hand this fluid dynamics scenario does not lead to a simultaneous and quantitative understanding of clusterization, momentum-space population and size dependences. Since, furthermore, nonequilibrium effects were shown directly to be important in a mixing experiment, it seems clear that transport calculations are necessary in order to understand the dynamics and eventually draw more 'fundamental' conclusions about the acting nuclear forces and the equation of state.

References

1. W. Reisdorf *et al*, *Nucl. Phys.* A **612**, 493 (1997).
2. S.C. Jeong *et al*, *Phys. Rev. Lett.* **72**, 3468 (1994).
3. M. Petrovici *et al*, *Phys. Rev. Lett.* **74**, 5001 (1995).
4. A. Ono , contribution this conference.
5. A. Gobbi *et al*, *Nucl. Instrum. Methods* A **324**, 156 (1993),
   J. Ritman *et al*, *Nucl. Phys.* B **44**, 708 (1995).
6. A. Schüttauf *et al*, *Nucl. Phys.* A **607**, 457 (1996).
7. F. Rami, contribution this conference.
8. B. de Schauenburg, Ph. D. thesis, Strasbourg (1999),
   F. Rami, Y. Leifels, B. de Schauenburg, A. Gobbi *et al*, to be published.